Oversampling-Based Algorithm for Efficient RF Interference Excision in SIMO Systems

Tilahun Melkamu Getu[†‡], Wessam Ajib[‡] and René Jr. Landry[†]
[†]École de Technologie Supérieure (ÉTS), Montréal, QC, Canada
[‡]Université du Québec À Montréal (UQÀM), Montréal, QC, Canada
tilahun-melkamu.getu.1@ens.etsmtl.ca, ajib.wessam@uqam.ca and renejr.landry@etsmtl.ca

***Abstract*—For intentional or unintentional interferers, radio frequency interference (RFI) is being prevalent in both satellite and terrestrial communications. In this regard, efficient RFI excision algorithms would have a paramount importance. Having relied on recent advances in tensor-based signal processing, the paper proposes oversampled multi-linear subspace estimation and projection (o-MLSEP) algorithm for efficient multi-interferer RFI (MI-RFI) excision in single-input multiple-output (SIMO) systems. Simulations corroborate that o-MLSEP significantly improves MLSEP as the oversampling factor gets larger.**

***Index Terms*—RFI, RFI excision, oversampling, multi-linear subspace estimation, multi-linear projection.**

I. Introduction

Radio frequency interference (RFI) is generally caused by out-of-band emissions by nearby transmitters and harmonics, jamming, spoofing and meaconing. If left unmitigated, such RFI can evoke a severe system performance loss in both satellite and terrestrial communications. As a result, spectral [1], temporal [2], spectral-temporal [3], transformed domain-based [4], statistical [5] and spatial filtering-based [6] [7] RFI detection and excision algorithms have been proposed for radio astronomy, microwave radiometry and global navigation satellite system (GNSS) applications.

Having relied on recent advances in tensor-based signal processing [8] [9], we have introduced the multi-linear algebra framework to the RFI excision research in [10] by proposing the multi-linear subspace estimation and projection (MLSEP) algorithm for RFI excision in single-input multiple-output (SIMO) systems. Meanwhile, this paper proposes the oversampled MLSEP (o-MLSEP) algorithm for efficient multi-interferer RFI (MI-RFI) excision in SIMO systems.

Oversampled antenna arrays have been deployed to improve the performance of the tensor-based channel estimation algorithm proposed in [11]. Similarly, we believe that oversampled antenna arrays can be exploited in the estimation of the MI-RFI subspace. Higher-order singular value decomposition (HOSVD) is used for the estimation of the oversampled MI-RFI subspace while maintaining the inherent structure of the measurement data. Thereafter, the oversampled multi-linear projector which evokes perfect excision of the MI-RFI is derived and an MI-RFI excision is performed afterwards. Following this introduction, Section II presents the notation and system model. Section III details the o-MLSEP algorithm. Simulation results are then presented in Section IV followed by paper conclusions which are drawn in Section V.

II. Notation and System Model

A. Notation

The notations $\sim$, $(:,i)$, $||\cdot||_F$, $(\cdot)^T$, $(\cdot)^H$, $\otimes$, $(\cdot)^{+r}$, $\min(\cdot,\cdot)$, $\mathbb{E}\{\cdot\}$ and $\mathcal{N}(\cdot,\cdot)$ imply distributed as, the ith column of a matrix, Frobenius norm, transposition, Hermitian transposition, Kronecker product, the r-mode pseudo-inverse of a tensor, minimum, expectation and normal distribution, respectively. Besides, the horizontal concatenation of matrices $\boldsymbol{A}$ and $\boldsymbol{B}$ is denoted as $[\boldsymbol{A}, \boldsymbol{B}]$.

The tensor $\boldsymbol{\mathcal{A}} \in \mathbb{C}^{I_1 \times I_2 \times \ldots \times I_R}$ is an R-way array of size I_r along the r-th mode consistent with [12]. The r-mode vectors of $\boldsymbol{\mathcal{A}}$ are obtained by varying the rth index, while keeping all other indices fixed. The r-mode unfolding of $\boldsymbol{\mathcal{A}}$ is obtained by collecting all r-mode vectors into a matrix and represented by $[\boldsymbol{\mathcal{A}}]_{(r)} \in \mathbb{C}^{I_r \times I_{r+1} \cdot \ldots \cdot I_R \cdot I_1 \cdot \ldots \cdot I_{r-1}}$ [11]. The r-rank of $\boldsymbol{\mathcal{A}}$ is defined as the rank of $[\boldsymbol{\mathcal{A}}]_{(r)}$. The r-mode product of $\boldsymbol{\mathcal{A}}$ and a matrix $\boldsymbol{U}_r \in \mathbb{C}^{J_r \times I_r}$ is denoted as $\boldsymbol{\mathcal{B}} = \boldsymbol{\mathcal{A}} \times_r \boldsymbol{U}_r$ and defined through $[\boldsymbol{\mathcal{B}}]_{(r)} = \boldsymbol{U}_r [\boldsymbol{\mathcal{A}}]_{(r)}$ [8]. Similarly, the r-mode product of $\boldsymbol{\mathcal{A}}$ and a tensor $\boldsymbol{\mathcal{C}} \in \mathbb{C}^{J_1 \times J_2 \times \ldots J_r \times \ldots \times J_R}$, where $I_r = J_1 J_2 \ldots J_{r-1} J_{r+1} \ldots J_R$, is denoted by $\boldsymbol{\mathcal{D}} = \boldsymbol{\mathcal{A}} \times_r \boldsymbol{\mathcal{C}} \in \mathbb{C}^{I_1 \times \ldots I_{r-1} \times J_r \times I_{r+1} \ldots \times I_R}$ and defined through $[\boldsymbol{\mathcal{D}}]_{(r)} = [\boldsymbol{\mathcal{C}}]_r [\boldsymbol{\mathcal{A}}]_{(r)}$ [13]. Accordingly, the r-mode identity tensor $\boldsymbol{\mathcal{I}}_r \in \mathbb{C}^{J_1 \times J_2 \times \ldots J_r \times \ldots \times J_R}$ as well as the r-mode pseudo-inverse tensor $\boldsymbol{\mathcal{A}}^{+r}$ satisfy [13]

$$\left(\boldsymbol{\mathcal{A}} \times_r \boldsymbol{\mathcal{A}}^{+r}\right) \times_r \boldsymbol{\mathcal{A}} = \boldsymbol{\mathcal{A}} \text{ and } \boldsymbol{\mathcal{I}}_r \times_r \boldsymbol{\mathcal{A}} = \boldsymbol{\mathcal{A}}, \tag{1}$$

where $[\boldsymbol{\mathcal{A}}^{+r}]_{(r)} = [\boldsymbol{\mathcal{A}}]^{+}_{(r)}$, $[\boldsymbol{\mathcal{I}}]_{(r)} = \boldsymbol{I}_{J_r \times J_{r+1} \ldots J_R J_1 \ldots J_{r-1}}$, $J_r = J_{r+1} \ldots J_R J_1 \ldots J_{r-1}$ and $J_r = I_{r+1} \ldots I_R I_1 \ldots I_{r-1}$.

B. System Model

A SIMO system suffering from severe MI-RFI emitted by Q independent single-antenna interferers is considered. The signal of interest (SOI) channel between the transmitter and each receive antenna pair is modeled as a finite-duration impulse response (FIR) filter with $L+1$ taps. The SOI channel is assumed to be time-invariant for a long-term interval (LTI). Similarly, the RFI channel between the ith RFI transmitter and each receive antenna pair is modeled as an FIR filter with $L_i + 1$, $1 \leq i \leq Q$, taps. Meanwhile, the MI-RFI channel is presumed to have a coherence time of $N_{\text{SOI}} + 1$ times the coherence time of the SOI—N_{SOI} being an arbitrary constant. The received signal at time n will then be

$$\boldsymbol{y}(n) = \sum_{l=0}^{L} \boldsymbol{h}_l s(n-l) + \sum_{i=1}^{Q}\sum_{l=0}^{L_i} \boldsymbol{g}_i^{(l)} f_i(n-l) + \boldsymbol{z}(n), \quad (2)$$

where $\{\boldsymbol{h}_l, \boldsymbol{g}_i^{(l)}\} \in \mathbb{C}^{N_R}$ are the array response of the N_R antennas corresponding to the lth SOI and the ith RFI's lth channel tap, respectively, $s(n)$ denotes the symbol emitted by the SOI transmitter at time n, $f_i(n)$ is the sampled ith broadband RFI which is usually modeled as a zero mean additive white Gaussian noise (AWGN) [14] and $\boldsymbol{z}(n) \sim \mathcal{N}(\boldsymbol{0}, \sigma^2 \boldsymbol{I}_{N_R})$ is a sampled AWGN. Moreover, we assume that the SOI, Q RFIs and noise are uncorrelated and perfect estimates of L, Q and L_i, $1 \le i \le Q$, are available.

III. o-MLSEP: Oversampled MLSEP

In the o-MLSEP detailed subsequently, oversampled antenna arrays are used in the MI-RFI subspace estimation tensor which is estimated in the first LTI while transmitting no SOI. An LTI is made of N short-term intervals (STIs). Each STI has a duration of WT_s for T_s being the symbol duration. From the estimated MI-RFI subspace tensor, the projection tensor which is used for an MI-RFI excision is derived. From the second LTI onwards, SOI will be transmitted for an N_{SOI} LTIs and a per LTI MI-RFI excision will be conducted.

A. Problem Setup

Stacking W samples from every N_R antennas with respect to the mth STI results in the measurement data as

$$\boldsymbol{y}_m = \boldsymbol{H}\boldsymbol{s}_m + \boldsymbol{G}\boldsymbol{f}_m + \boldsymbol{z}_m \in \mathbb{C}^{N_R W}, \quad (3)$$

where $\boldsymbol{s}_m = \big[s(mW), \ldots, s(mW - W - L + 1)\big]^T$, $\boldsymbol{f}_m = [\boldsymbol{f}_{1m}^T, \ldots, \boldsymbol{f}_{Qm}^T]^T \in \mathbb{C}^{\sum_{i=1}^{Q}(W+L_i)}$ for $\boldsymbol{f}_{im} = \big[f_i(mW), \ldots, f_i(mW - W - L_i + 1)\big]^T$—$1 \le i \le Q$—and $\boldsymbol{z}_m$ are the sampled SOI, MI-RFI and a zero mean AWGN, respectively. Besides, $\boldsymbol{H} \in \mathbb{C}^{N_R W \times (W+L)}$ is the SOI filtering matrix in [11, eq. (3) & (5)] and $\boldsymbol{G} = [\boldsymbol{G}_1, \boldsymbol{G}_2, \ldots, \boldsymbol{G}_Q] \in \mathbb{C}^{N_R W \times \sum_{i=1}^{Q}(W+L_i)}$ is the MI-RFI filtering matrix for $\boldsymbol{G}_i$, $1 \le i \le Q$, being the ith RFI filtering matrix structured as

$$\boldsymbol{G}_i = \Big[\boldsymbol{G}_{i1}^T, \boldsymbol{G}_{i2}^T, \ldots, \boldsymbol{G}_{iN_R}^T\Big]^T. \quad (4)$$

In (4), $\boldsymbol{G}_{ij} \in \mathbb{C}^{W \times (W+L_i)}$ is a banded Toeplitz matrix associated with the ith RFI and the jth receive antenna's impulse response $\boldsymbol{g}_{ij} \triangleq \big[g_{ij}^0, g_{ij}^1, \ldots, g_{ij}^{L_i}\big]^T = \big[g_{ij}(t_0), g_{ij}(t_0 + T_s), \ldots, g_{ij}(t_0 + L_i T_s)\big]^T$—$t_0$ being the time-of-arrival—and

$$\boldsymbol{G}_{ij} = \begin{bmatrix} g_{ij}^0 & \ldots & g_{ij}^{L_i} & 0 & \ldots & \ldots & 0 \\ 0 & g_{ij}^0 & \ldots & g_{ij}^{L_i} & 0 & \ldots & 0 \\ \vdots & \vdots & \vdots & \vdots & \vdots & \vdots & \vdots \\ 0 & \ldots & \ldots & 0 & g_{ij}^0 & \ldots & g_{ij}^{L_i} \end{bmatrix}. \quad (5)$$

The horizontal concatenation of N $\boldsymbol{y}_m$s from (3) renders

$$\boldsymbol{Y} = \boldsymbol{H}\boldsymbol{S} + \boldsymbol{G}\boldsymbol{F} + \boldsymbol{Z} \in \mathbb{C}^{N_R W \times N}, \quad (6)$$

where $\boldsymbol{S} = [\boldsymbol{s}_1, \ldots, \boldsymbol{s}_N]$, $\boldsymbol{F} = [\boldsymbol{F}_1^T, \ldots, \boldsymbol{F}_Q^T]^T$, $\boldsymbol{F}_i = [\boldsymbol{f}_{i1}, \ldots, \boldsymbol{f}_{iN}] \in \mathbb{C}^{(W+L_i)\times N}$, $1 \le i \le Q$, and $\boldsymbol{Z} = [\boldsymbol{z}_1, \ldots, \boldsymbol{z}_N]$. For the oversampling time interval of T_s^o, oversampling (6) by a factor of $O = T_s / T_s^o$ generates

$$\boldsymbol{Y}^o = \boldsymbol{H}^o \boldsymbol{S} + \boldsymbol{G}^o \boldsymbol{F} + \boldsymbol{Z}^o \in \mathbb{C}^{N_R O W \times N}, \quad (7)$$

where $\boldsymbol{H}^o \in \mathbb{C}^{N_R O W \times (W+L)}$ is the oversampled SOI filtering matrix in [11, eq. (14)], $\boldsymbol{G}^o = [\boldsymbol{G}_1^o, \boldsymbol{G}_2^o, \ldots, \boldsymbol{G}_Q^o] \in \mathbb{C}^{N_R O W \times \sum_{i=1}^{Q}(W+L_i)}$ is the oversampled MI-RFI filtering matrix for $\boldsymbol{G}_i^o = \big[\boldsymbol{G}_{i10}^T, \boldsymbol{G}_{i11}^T, \ldots, \boldsymbol{G}_{i1(O-1)}^T, \boldsymbol{G}_{i20}^T, \boldsymbol{G}_{i21}^T, \ldots, \boldsymbol{G}_{iN_R(O-1)}^T\big]^T \in \mathbb{C}^{N_R O W \times (W+L_i)}$ being the ith oversampled RFI filtering matrix and $\boldsymbol{G}_{ijo}$, $1 \le i \le Q$, $1 \le j \le N_R$, $1 \le o \le O-1$, being a banded Toeplitz matrix and $\boldsymbol{Z}^o$ is an oversampled noise matrix. Due to oversampling, both the noise [11] and the Gaussian MI-RFI samples become *temporally correlated.* Furthermore, the banded Toeplitz matrix $\boldsymbol{G}_{ijo}$ is made of $\boldsymbol{g}_{ijo}$ defined as $\boldsymbol{g}_{ijo} \triangleq \Big[g_{ij}(t_0 + oT_s^o), \ldots, g_{ij}(t_0 + oT_s^o + L_i T_s)\Big]^T$ and hence $\boldsymbol{g}_{ij0} = \boldsymbol{g}_{ij}$. In the first LTI, no SOI is transmitted and the oversampled received signal be $\boldsymbol{Y}_I^o = \boldsymbol{G}^o \boldsymbol{F} + \boldsymbol{Z}^o$. The SVD of $\boldsymbol{Y}_I^o$ provides the estimated oversampled MI-RFI subspace $\hat{\boldsymbol{U}}_I^o \in \mathbb{C}^{N_R O W \times \sum_{i=1}^{Q}(W+L_i)}$ as

$$\boldsymbol{Y}_I^o = [\hat{\boldsymbol{U}}_I^o \;\; \hat{\boldsymbol{U}}_n^o] \begin{bmatrix} \hat{\boldsymbol{\Sigma}}_I^o & \boldsymbol{0}_{r\times(N-r)} \\ \boldsymbol{0}_{(N_R O W - r)\times r} & \hat{\boldsymbol{\Sigma}}_n^o \end{bmatrix} [\hat{\boldsymbol{V}}_I^o \;\; \hat{\boldsymbol{V}}_n^o]^H, \quad (8)$$

where $\hat{\boldsymbol{\Sigma}}_I^o = \text{diag}(\sigma_1^o, \ldots, \sigma_r^o)$ and $r = \sum_{i=1}^{Q}(W + L_i)$.

B. Problem Formulation

We first model the oversampled received signal by a three-way tensor $\boldsymbol{\mathcal{Y}}^o \in \mathbb{C}^{N_R O \times W \times N}$. Should $\Big[\boldsymbol{\mathcal{Y}}^o\Big]_{(3)}^T$ be equal to $\boldsymbol{Y}^o$ in (7), the multi-linear equivalent of (7) will be

$$\boldsymbol{\mathcal{Y}}^o = \boldsymbol{\mathcal{H}}^o \times_3 \boldsymbol{S}^T + \boldsymbol{\mathcal{G}}^o \times_3 \boldsymbol{F}^T + \boldsymbol{\mathcal{Z}}^o, \quad (9)$$

where $\boldsymbol{\mathcal{H}}^o \in \mathbb{C}^{N_R O \times W \times (W+L)}$ and $\boldsymbol{\mathcal{G}}^o \in \mathbb{C}^{N_R O \times W \times r}$ are the oversampled SOI and MI-RFI filtering tensors constructed by aligning the banded Toeplitz matrices $\boldsymbol{H}_{jo}$ and $\boldsymbol{G}_{ijo}$ along the first dimension, respectively, as in Fig. 1, i.e., $[\boldsymbol{\mathcal{H}}^o]_{(3)}^T = \boldsymbol{H}^o$ and $[\boldsymbol{\mathcal{G}}^o]_{(3)}^T = \boldsymbol{G}^o$, and $\boldsymbol{\mathcal{Z}}^o$ is the oversampled noise tensor. Meanwhile, we assume that $\boldsymbol{S}$ has a rank of $W + L$, i.e., $N \ge (W + L)$, $\boldsymbol{F}$ has a rank of r, i.e., $N \ge r$, $[\boldsymbol{\mathcal{H}}^o]_{(3)}$ has a full row rank, i.e., $N_R O W \ge W + L$, $[\boldsymbol{\mathcal{G}}^o]_{(3)}$ has a full row rank, i.e., $N_R O W \ge r$, $W > L$ and $W > L_i$, $1 \le i \le Q$, in order to ensure the identifiability of the SOI and oversampled MI-RFI subspaces [10].

1) Oversampled MI-RFI Subspace Estimation: In the first LTI, the truncated HOSVD of the received signal $\boldsymbol{\mathcal{Y}}_{\boldsymbol{I}}^o = \boldsymbol{\mathcal{G}}^o \times_3 \boldsymbol{F}^T + \boldsymbol{\mathcal{Z}}^o$ will be [9, eq. (16)]

$$\boldsymbol{\mathcal{Y}}_I^o \approx \hat{\boldsymbol{\mathcal{S}}}^{o[I]} \times_1 \hat{\boldsymbol{U}}_1^{o[I]} \times_2 \hat{\boldsymbol{U}}_2^{o[I]} \times_3 \hat{\boldsymbol{U}}_3^{o[I]}, \quad (10)$$

where $\hat{\boldsymbol{\mathcal{S}}}^{o[I]} \in \mathbb{C}^{r_1^o \times r_2^o \times r_3^o}$ is the core tensor which satisfies the all-orthogonality conditions, $\hat{\boldsymbol{U}}_1^{o[I]} \in \mathbb{C}^{N_R O \times r_1^o}$ is a unitary matrix of the singular vectors of $[\boldsymbol{\mathcal{Y}}_I^o]_{(1)}$, $\hat{\boldsymbol{U}}_2^{o[I]} \in \mathbb{C}^{W \times r_2^o}$ is a unitary matrix of the singular vectors of $[\boldsymbol{\mathcal{Y}}_I^o]_{(2)}$, $\hat{\boldsymbol{U}}_3^{o[I]} \in$

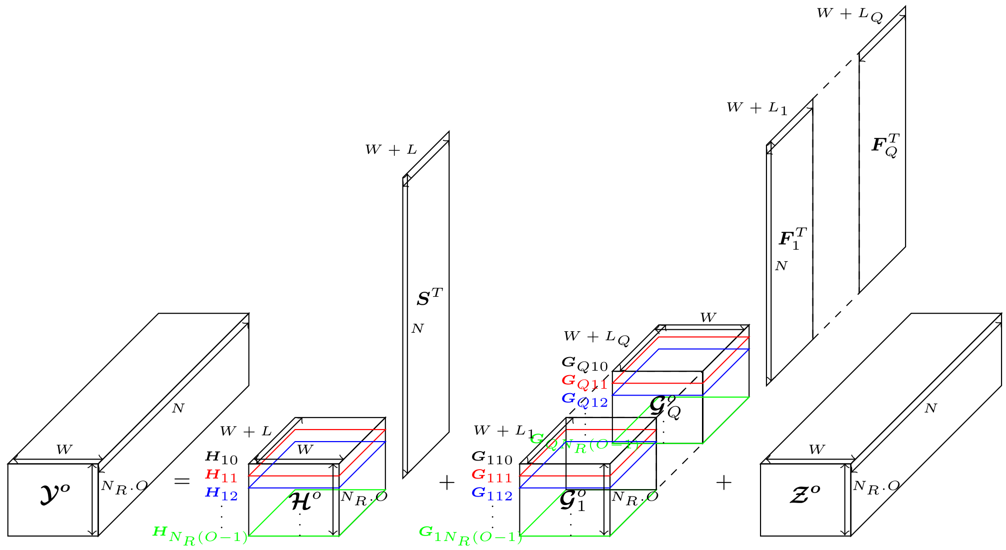

Fig. 1. Multi-linear formulation from (7).

$\mathbb{C}^{N\times r_3^o}$ is a unitary matrix of the singular vectors of $[\mathcal{Y}_I^o]_{(3)}$ and r_n^o denotes the n-rank of $\widetilde{\mathcal{Y}}_I^o = \mathcal{G}^o \times_3 \boldsymbol{F}^T$ for $n \in \{1,2,3\}$ [9]. In our estimation, $r_1^o = \min\big(N_R O,\ \sum_{i=1}^{Q}(L_i+1)\big)$, $r_2^o = \min(W,\ NN_R)$ and $r_3^o = \min\big(N,\ r\big)$. Accordingly, $r_2^o = W$ and $r_3^o = r$ for $N \geq r$. The estimated oversampled MI-RFI subspace tensor $\hat{\mathcal{U}}^{o[I]}$ is then defined as [9, eq. (17)]

$$\hat{\mathcal{U}}^{o[I]} = \hat{\mathcal{S}}^{o[I]} \times_1 \hat{\boldsymbol{U}}_1^{o[I]} \times_2 \hat{\boldsymbol{U}}_2^{o[I]} \times_3 \hat{\boldsymbol{\Sigma}}_I^{o-1}. \quad (11)$$

Note that the columns of $\left[\hat{\mathcal{U}}^{o[I]}\right]_{(3)}^T \in \mathbb{C}^{N_R OW\times r_3^o}$ span the estimated MI-RFI subspace and inspire the succeeding theorem.

Theorem 1: The tensor-based oversampled MI-RFI subspace estimator $\left[\hat{\mathcal{U}}^{o[I]}\right]_{(3)}^T$ and the matrix-based oversampled MI-RFI subspace estimator $\hat{\boldsymbol{U}}_I^o$ are related by

$$\left[\hat{\mathcal{U}}^{o[I]}\right]_{(3)}^T = \left(\hat{\boldsymbol{T}}_1^o \otimes \hat{\boldsymbol{T}}_2^o\right)\hat{\boldsymbol{U}}_I^o, \quad (12)$$

where $\hat{\boldsymbol{T}}_r^o = \hat{\boldsymbol{U}}_r^{o[I]}\hat{\boldsymbol{U}}_r^{o[I]^H}$, $r \in \{1,2\}$.

Proof: Following [9, Theorem 1], Theorem 1 can be proved for $R=2$ and $\hat{\boldsymbol{T}}_r^o = \hat{\boldsymbol{T}}_r$, $r \in \{1,2\}$. ∎

2) Oversampled Multi-Linear Projection: The theorem below is valid for a perfectly estimated MI-RFI subspace tensor.

Theorem 2: For a perfectly estimated $\hat{\mathcal{U}}^{o[I]} \in \mathbb{C}^{N_R O\times W\times r}$, the oversampled multi-linear projector $\mathcal{P}^o \in \mathbb{C}^{N_R O\times W\times N_R OW}$ which evokes perfect excision of the oversampled MI-RFI is given by

$$\mathcal{P}^o = \mathcal{I}_3^o - \hat{\mathcal{U}}^{o[I]} \times_3 \left(\hat{\mathcal{U}}^{o[I]}\right)^{+3}, \quad (13)$$

where $\mathcal{I}_3^o \in \mathbb{C}^{N_R O\times W\times N_R OW}$ is the 3-mode identity tensor, $\left(\hat{\mathcal{U}}^{o[I]}\right)^{+3}$ is the 3-mode pseudo-inverse tensor, $[\mathcal{I}_3^o]_{(3)} = \boldsymbol{I}_{N_R OW}$ and $\left[\left(\hat{\mathcal{U}}^{o[I]}\right)^{+3}\right]_{(3)} = \left[\hat{\mathcal{U}}^{o[I]}\right]_{(3)}^{+}$.

Proof: cf. Appendix A. ∎

Nonetheless, $\hat{\mathcal{U}}^{o[I]}$ cannot be perfect and we make use of the root mean square excision error (RMSEE) parameter as

$$\text{RMSEE} = \sqrt{\mathbb{E}\Big\{\big\|\left[\mathcal{P}^o \times_3 \mathcal{G}^o\right]_{(3)}^T\big\|_F^2\Big\}}. \quad (14)$$

Meanwhile, the underneath Algorithm I summarizes the proposed o-MLSEP algorithm for $N_{\text{tot}} = WN$ being the number of observed symbols per LTI .

Algorithm I: o-MLSEP for efficient MI-RFI excision in SIMO systems

Input: $\boldsymbol{Y}_I^o$, $\boldsymbol{Y}^o$, N_R, W, N, Q, L_f^i, $1 \leq i \leq Q$, O
Assumptions: All assumptions of Sec. III-B
Initializations: Defined ranks of Sec. III-B

```
    Y_I^o =the tensorization of [Y_I^o]_(3) = Y_I^oT
    Computation and tensorization of (12)
    Computation of P^o using (13)
Repeat
    Y^o =the tensorization of [Y^o]_(3) = Y^oT
    return [P^o ×_3 Y^o]^T_(3)
Until N_SOI LTIs
```

IV. Simulation Results

During the first LTI, Q zero mean white Gaussian signals which model the broadband MI-RFI are transmitted over a multipath fading channel. From the second LTI onwards, both Gray-coded 4-QAM symbols and Q white Gaussian signals are transmitted over multipath fading channels for 200 LTIs. To simulate the SOI and each RFI multipath fading channels, $(L+1)$- and (L_i+1)-ray multipath continuous-time channels are constructed synchronously using the raised cosine pulse shaping filter $p_{rc}(t,\beta)$ with a roll-off factor of $\beta = 0.5$ and propagation delay $t_0 = 0.1T_s$ as in [11] and [15]. Then the constructed channels are oversampled and o-MLSEP is simulated as per Algorithm I by employing the succeeding simulation setup.

$\boldsymbol{H}$ and $\boldsymbol{G}_i$ are normalized to a Frobenius norm of $\sqrt{W}$. A temporally correlated noise and MI-RFI—with correlation matrices of $\boldsymbol{R}_{nn}$ and $\boldsymbol{R}_{ff}$, respectively—are generated. Signal-to-interference-plus-noise ratio (SINR) in dB which is denoted as $\gamma_{sinr}(\boldsymbol{P}^o)$, average SINR gain [dB] and interference-to-noise ratio (INR) in dB which is denoted as γ_{inr} are defined, respectively, as $\gamma_{sinr}(\boldsymbol{P}^o) = 10\log_{10}\frac{\mathbb{E}\left\{\left\|\boldsymbol{P}^o\boldsymbol{H}^o\boldsymbol{S}\right\|_F^2\right\}}{\mathbb{E}\left\{\left\|\boldsymbol{P}^o\boldsymbol{G}\boldsymbol{F}\right\|_F^2\right\}+\mathbb{E}\left\{\left\|\boldsymbol{P}^o\boldsymbol{Z}^o\right\|_F^2\right\}}$, $\frac{1}{N_{\text{SOI}}}\sum_{n=1}^{N_{\text{SOI}}}\left(\gamma_{sinr}(\boldsymbol{P}^o) - \gamma_{sinr}(\boldsymbol{I}_{N_ROW})\right)$ and $\gamma_{inr} = 10\log_{10}\frac{\mathbb{E}\left\{\left\|\boldsymbol{G}^o\boldsymbol{F}\right\|_F^2\right\}}{\mathbb{E}\left\{\left\|\boldsymbol{Z}^o\right\|_F^2\right\}}$ for Q independent interferers with identical power. Furthermore, average normalized RMSEE (NRMSEE) is simulated by averaging (14) normalized by the total number of elements in $[\boldsymbol{\mathcal{P}}^o \times_3 \boldsymbol{\mathcal{G}}^o]_{(3)}$ and Tensorlab [16] is used for our matricization and tensorization operations. Finally, Monte-Carlo simulations with parameters tabulated in Table I, unless otherwise mentioned, produced Figs. 2–5.

Simulation parameters	Assigned value
$[L, L_1, L_2, L_3]$	$[1, 1, 1, 1]$
$[W, N]$	$[5, 40]$
N_{tot}	200
N_{SOI}	200 LTIs
$[\boldsymbol{R}_{nn}]_{km}, [\boldsymbol{R}_{ff}]_{km}$	$[0.05, 0.05],\ k \neq m$
$[\boldsymbol{R}_{nn}]_{kk}, [\boldsymbol{R}_{ff}]_{kk}$	$[1, 1]$
No. of channel realizations	500

TABLE I
SIMULATION PARAMETERS UNLESS OTHERWISE MENTIONED.

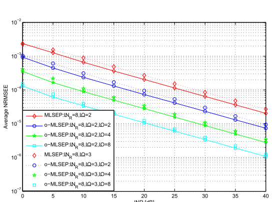

Fig. 2. Comparison in average NRMSEE for a pre-excision SINR of 0 dB.

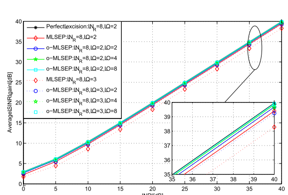

Fig. 3. Comparison in average SINR gain for a pre-excision SINR of 0 dB.

Fig. 2 showcases o-MLSEP outperforming MLSEP especially for larger oversampling factor O, since the oversampled MI-RFI subspace estimating tensor in (11) renders a better MI-RFI subspace estimation accuracy. Meanwhile, the aforementioned improvement in accuracy is translated to the average SINR gain depicted in Fig. 3. Similarly, Fig. 4 and Fig. 5 corroborate the performance improvement of o-MLSEP with respect to N_R.

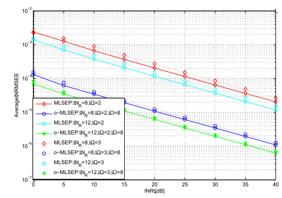

Fig. 4. Comparison in average NRMSEE for a pre-excision SINR of 0 dB.

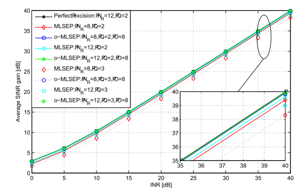

Fig. 5. Comparison in average SINR gain for a pre-excision SINR of 0 dB.

V. CONCLUSIONS

The paper enhances the MLSEP algorithm by deploying oversampled antenna arrays. To do so, truncated HOSVD is used to estimate the oversampled MI-RFI subspace tensor. Then, the multi-linear projector that renders perfect excision of the MI-RFI for the perfectly estimated MI-RFI subspace tensor is derived. The aforementioned oversampled multi-linear subspace estimation and projection produced the o-MLSEP algorithm. Finally, Monte-Carlo simulations have corroborated that o-MLSEP outperforms MLSEP as the oversampling factor gets larger though at the cost of oversampling complexity and O times number of multiplications.

APPENDIX A
PROOF OF THEOREM 2

Proof: For a perfect $\hat{\boldsymbol{\mathcal{U}}}^{o[I]}$, the MI-RFI in (9) will be perfectly removed via $\boldsymbol{\mathcal{P}}^o \in \mathbb{C}^{N_RO\times W\times N_ROW}$ if and only if

$$\boldsymbol{\mathcal{P}}^o \times_3 \hat{\boldsymbol{\mathcal{U}}}^{o[I]} = \boldsymbol{\mathcal{P}}^o \times_3 \boldsymbol{\mathcal{G}}^o = \boldsymbol{\mathcal{O}}_t^o = \hat{\boldsymbol{\mathcal{U}}}^{o[I]} - \hat{\boldsymbol{\mathcal{U}}}^{o[I]}, \quad (15)$$

where $\boldsymbol{\mathcal{O}}_t^o \in \mathbb{C}^{N_R.O\times W\times r}$ is a zero tensor. From (1), $\left(\hat{\boldsymbol{\mathcal{U}}}^{o[I]} \times_3 \left(\hat{\boldsymbol{\mathcal{U}}}^{o[I]}\right)^{+3}\right) \times_3 \hat{\boldsymbol{\mathcal{U}}}^{o[I]} = \hat{\boldsymbol{\mathcal{U}}}^{o[I]}$ and $\boldsymbol{\mathcal{I}}_3^o \times_3 \hat{\boldsymbol{\mathcal{U}}}^{o[I]} = \hat{\boldsymbol{\mathcal{U}}}^{o[I]}$. Thus, perfect excision is possible iff

$$\boldsymbol{\mathcal{P}}^o \times_3 \hat{\boldsymbol{\mathcal{U}}}^{o[I]} = \boldsymbol{\mathcal{I}}_3^o \times_3 \hat{\boldsymbol{\mathcal{U}}}^{o[I]} - \left(\hat{\boldsymbol{\mathcal{U}}}^{o[I]} \times_3 \left(\hat{\boldsymbol{\mathcal{U}}}^{o[I]}\right)^{+3}\right) \times_3 \hat{\boldsymbol{\mathcal{U}}}^{o[I]}. \quad (16)$$

Applying the definition of r-mode product (cf. Section II) and the distributive property of matrix product to (16) results in

$$\left[\boldsymbol{\mathcal{P}}^o \times_3 \hat{\boldsymbol{\mathcal{U}}}^{o[I]}\right]_{(3)} = \left[\hat{\boldsymbol{\mathcal{U}}}^{o[I]}\right]_{(3)} \cdot \left(\left[\boldsymbol{\mathcal{I}}_3^o\right]_{(3)} - \left[\hat{\boldsymbol{\mathcal{U}}}^{o[I]} \times_3 \left(\hat{\boldsymbol{\mathcal{U}}}^{o[I]}\right)^{+3}\right]_{(3)}\right). \quad (17)$$

Thereafter, the tensorization of (17) renders

$$\boldsymbol{\mathcal{P}}^o \times_3 \hat{\boldsymbol{\mathcal{U}}}^{o[I]} = \left(\boldsymbol{\mathcal{I}}_3^o - \hat{\boldsymbol{\mathcal{U}}}^{o[I]} \times_3 \left(\hat{\boldsymbol{\mathcal{U}}}^{o[I]}\right)^{+3}\right) \times_3 \hat{\boldsymbol{\mathcal{U}}}^{o[I]}. \quad (18)$$

Finally, it is easily deduced from (18) that

$$\boldsymbol{\mathcal{P}}^o = \boldsymbol{\mathcal{I}}_3^o - \hat{\boldsymbol{\mathcal{U}}}^{o[I]} \times_3 \left(\hat{\boldsymbol{\mathcal{U}}}^{o[I]}\right)^{+3}. \quad (19)$$

■

REFERENCES

[1] B. Guner, J. Johnson, and N. Niamsuwan, “Time and frequency blanking for radio-frequency interference mitigation in microwave radiometry,” *IEEE Trans. Geosci. Remote Sens.*, vol. 45, no. 11, pp. 3672–3679, Nov. 2007.

[2] J. T. Johnson and S. W. Ellingson, “Examination of a simple pulse blanking technique for RFI mitigation,” *Wiley Radio Sci.*, 2005.

[3] D. Borio, L. Camoriano, S. Savasta, and L. Lo Presti, “Time-frequency excision for GNSS applications,” *IEEE Syst. J.*, vol. 2, no. 1, pp. 27–37, Mar. 2008.

[4] F. Dovis, L. Musumeci, N. Linty, and M. Pini, “Recent trends in interference mitigation and spoofing detection,” *Int. J. of Embedded and Real-Time Commun. Systems*, vol. 3, no. 3, pp. 1–17, July-Sept. 2012.

[5] C. Ruf, S. Gross, and S. Misra, “RFI detection and mitigation for microwave radiometry with an agile digital detector,” *IEEE Trans. Geosci. Remote Sens.*, vol. 44, no. 3, pp. 694–706, Mar. 2006.

[6] S. van der Tol and A.-J. van der Veen, “Performance analysis of spatial filtering of RF interference in radio astronomy,” *IEEE Trans. Signal Process.*, vol. 53, no. 3, pp. 896–910, Mar. 2005.

[7] B. Jeffs, L. Li, and K. F. Warnick, “Auxiliary antenna-assisted interference mitigation for radio astronomy arrays,” *IEEE Trans. Signal Process.*, vol. 53, no. 2, pp. 439–451, Feb. 2005.

[8] M. Haardt, F. Roemer, and G. Del Galdo, “Higher-order SVD-based subspace estimation to improve the parameter estimation accuracy in multidimensional harmonic retrieval problems,” *IEEE Trans. Signal Process.*, vol. 56, no. 7, pp. 3198–3213, July 2008.

[9] F. Roemer, M. Haardt, and G. Del Galdo, “Analytical performance assessment of multi-dimensional matrix- and tensor-based ESPRIT-type algorithms,” *IEEE Trans. Signal Process.*, vol. 62, no. 10, pp. 2611–2625, May 2014.

[10] T. M. Getu, W. Ajib, and O. Yeste, “Multi-linear subspace estimation and projection for efficient RFI excision in SIMO systems,” in *Proc. IEEE Global Conf. on Signal and Inform. Process. (IEEE GlobalSIP)*, Orlando, FL, USA, Dec. 2015, pp. 1397–1401.

[11] B. Song, F. Roemer, and M. Haardt, “Blind estimation of SIMO channels using a tensor-based subspace method,” in *Proc. the 44th Asilomar Conf. on Signals, Systems and Computers*, Nov. 2010, pp. 8–12.

[12] L. D. Lathauwer, B. D. Moor, and J. Vandewalle, “A multilinear singular value decomposition,” *SIAM J. Matrix Anal. Appl.*, vol. 21, pp. 1253–1278, 2000.

[13] M. Vasilescu and D. Terzopoulos, “Multilinear projection for appearance-based recognition in the tensor framework,” in *Proc. IEEE Int. Conf. on Comput. Vision (IEEE ICCV)*, Oct. 2007, pp. 1–8.

[14] M. Wildemeersch and J. Fortuny-Guasch, “Radio frequency interference impact assessment on global navigation satellite systems,” EC Joint Research Centre, Security Tech. Assessment Unit, Tech. Rep., Jan. 2010.

[15] E. Moulines, P. Duhamel, J. Cardoso, and S. Mayrargue, “Subspace methods for the blind identification of multichannel FIR filters,” *IEEE Trans. Signal Process.*, vol. 43, no. 2, pp. 516–525, Feb. 1995.

[16] L. Sorber, M. V. Barel and L. D. Lathauwer, “Tensorlab v2.0,” Jan. 2014. [Online]. Available: http://www.tensorlab.net/